Different Effects of Palmitoyl-L-carnitine and Palmitoyl-CoA on Mitochondrial Function in Rat Ventricular Myocytes

Different Effects of Palmitoyl-L-carnitine and Palmitoyl-CoA on Mitochondrial Function in Rat Ventricular Myocytes

Hiromutsu Tominaga, Hideki Katoh, Keiichi Odagiri, Yasuyo Takeuchi,

Hirotaka Kawashima, Masao Saotome, Tsuyoshi Urushida,

Hiroshi Satoh and Hideharu Hayashi

Internal Medicine III, Hamamatsu University School of Medicine,

1-20-1 Handayama, Higashi-ward, Hamamatsu 431-3192, Japan

RUNNING HEAD:

Fatty acid intermediates and mitochondrial function

CORRESPONDENCE:

Hideki Katoh MD. PhD,

Division of Cardiology, Internal Medicine III,

Hamamatsu University School of Medicine,

1-20-1 Handayama, Higashi ward, Hamamatsu 431-3192, Japan

TEL: +81-53-435-2267

FAX: +81-53-434-2910

E-mail: hkatoh@hama-med.ac.jp

Abstract

Although mitochondrial oxidative catabolism of fatty acid (FA) is a major energy source for the adult mammalian heart**,** cardiac lipotoxity resulting from elevated serum FA and enhanced FA use has been implicated in the pathogenesis of heart failure. To investigate the effects of the intermediates of FA metabolism, palmitoyl-L-carnitine (Pal-car) and palmitoyl-CoA (Pal-CoA), on mitochondrial function, we measured membrane potential ($\Delta\psi_m$), opening of the mitochondrial permeability transition pore (mPTP) and the production of reactive oxygen species (ROS) in saponin-treated rat ventricular myocytes with a laser scanning confocal microscope. Our results revealed that: 1) lower concentrations of Pal-car (1 and 5 μM) caused a slight hyperpolarization of $\Delta\psi_m$ (TMRE intensity increased to 115.5 ± 5.4 % and 110.7±1.6 % of the baseline, respectively. $p<0.05$) but did not open mPTP, 2) a higher concentration of Pal-car (10 μM) depolarized $\Delta\psi_m$ (TMRE intensity decreased to 61.9 ± 12.2 % of the baseline, $p<0.01$) and opened mPTP (calcein intensity decreased to 70.7 ± 2.8% of the baseline, $p<0.01$), 3) Pal-CoA depolarized $\Delta\psi_m$ without opening mPTP, and 4) only the higher concentration of Pal-car (10 μM) increased ROS generation (DCF intensity increased to 3.4 ± 0.3 fold of the baseline). We concluded that excessive exogenous intermediates of long chain saturated FA may disturb mitochondrial function in different ways between

Pal-car and Pal-CoA. The distinct mechanisms of the deteriorating effects of long chain FA on mitochondrial function are important for our understanding of the development of cardiac diseases in systemic metabolic disorders.

Keywords: Palmitoyl-L-carnitine and Palmitoyl CoA; mitochondrial membrane potential; mitochondrial permeability transition pore; ROS production

Introduction

Metabolic syndrome and insulin resistance are risk factors for cardiovascular diseases and are frequently accompanied by high serum fatty acid (FA) levels. Recent studies (**10, 35**) have suggested that these metabolic disorders are also related to the development of clinical heart failure without any coronary heart disease (**1**). High serum FA levels are accompanied by an increased prevalence of serious arrhythmia and could be linked to a higher mortality in patients with heart failure (**22**, **35**). Opie proposed the concept of 'metabolic vicious cycle' (**24**) where increasing insulin resistance and serum FA levels, as a consequence of the hyper-adrenergic state, could reduce myocardial energy efficiency in a failing heart (**1**).

In studies using transgenic mice or rat models of obesity and diabetes (**5**, **38**), it has been shown that the accumulation of lipids and related intermediates in cardiomyocytes can be a cause of cardiac lipotoxicity or cardiac cell death resulting in an impaired contractile function and cardiac hypertrophy. Although the role of metabolic alteration in the development of heart failure is not yet fully understood, it is suggested that cardiac lipotoxity as a result of enhanced FA metabolism plays an important role in the onset and development of clinical heart failure (**15**).

An overload of FA, specifically saturated long chain FA such as palmitic acid (PA), affects mitochondrial function and induces cardiomyocytes apoptosis (**32**). PA is converted to its coenzyme A ester form (palmitoyl-CoA; Pal-CoA) in the cytosol (**12**) and this Pal-CoA would be taken up by mitochondria as a carnitine ester form (palmitoyl-L-carnitine; Pal-car) immediately (**33**) and reconverted to Pal-CoA by carnitine palmitoyl-transferase II (CPT-II) in the mitochondrial matrix (**12**). In previous studies using isolated mitochondria (**13**, **25**) or cultured cells (**32**, **37**), PA and its intermediates (Pal-car and Pal-CoA) have been shown to affect mitochondrial membrane potential ($\Delta\psi_m$), mitochondrial permeability transition pore (mPTP), activity of the respiratory chain, and generation of reactive oxygen species (ROS). Among these, accumulation of Pal-car and Pal-CoA in the myocytes may have an impact on mitochondrial function in physiological conditions. However, little is known whether Pal-car and Pal-CoA cause distinct responses in $\Delta\psi_m$, mPTP, and ROS generation *in vivo*. Here, the aim of this study was to investigate the differences in effects of FA intermediates on mitochondrial function at the myocyte level. For this purpose, we perfused permeabilized ventricular myocytes with Pal-car or Pal-CoA and monitored $\Delta\psi_m$, opening of mPTP, and generation of ROS.

Materials and Methods

Cell isolation and permeabilization

This investigation conforms to the Guide for the Care and Use of Laboratory Animals Published by the US National Institutes of Health (NIH Publication No. 85-23, revised 1996). Isolated myocytes were obtained by enzymatic dissociation from male Sprague-Dawley rats (250-350 g) and cells were kept in modified Kraft-Brühe (KB) solution (**9**), which contained (mM) 40 KCl, 20 KH_2PO_4, 3 $MgCl_2$, 50 glutamic acid, 10 glucose, 10 HEPES, and 0.5 EGTA (pH was adjusted to 7.4 with KOH). Just before the experiments, cells were placed in a chamber and incubated with normal Tyrode solution, composed of (mM) 143 NaCl, 5.4 KCl, 0.5 $MgCl_2$, 0.25 NaH_2PO_4, 1 $CaCl_2$, 5.6 glucose and 5 HEPES (pH 7.4 with NaOH). All experiments were conducted at room temperature (25 °C) within 6 hours of cell isolation, and all samples were perfused with the solutions (approximately 3.0 ml/min) according to the protocol. The sarcolemmal membrane of cardiac myocytes were permeabilized by saponin (0.05 mg/ml) for 30 sec in a Ca^{2+}-free internal solution, which contained (mM) 50 KCl, 80 K-asparate, 2 Na-pyruvate, 20 HEPES, 3 $MgCl_2$-$6H_2O$, 2 Na_2ATP, 3 EGTA (pH 7.3 with KOH), and then saponin was removed by the continuous perfusion of a Ca^{2+}-free internal solution for 2 min. Experiments were performed with a laser scanning confocal microscope

(LSM 510, Karl-Zeiss) coupled to an inverted microscope (Axiovert S100, Karl-Zeiss) with a 63 × water-immersion objective lens ([NA] =1.3: Karl-Zeiss).

Measurement of membrane potential

For the measurement of $\Delta\psi_m$, permeabilized myocytes were loaded with a continuous perfusion of fluorescent indicator tetramethylrhodamine ethyl ester (TMRE: 10 nM). TMRE was excited at 543 nm with a helium-neon laser, and the emission signals were collected through a 560 nm long-pass filter. Data is presented as the % of TMRE signal before the application of drugs. Fluorescence intensity was integrated over regions of interest (25 × 25 pixels) excluding the nuclei and the edge of the cell.

Imaging of mPTP opening

To evaluate mPTP opening, myocytes were loaded with calcein/AM (1 μM) for 25 min, and then sarcolemmal membrane was permeabilized to remove cytoplasmic dyes. This method allows a selective loading of calcein in mitochondria. On the opening of mPTP, entrapped calcein is released from the mitochondrial matrix. Calcein was excited at 488 nm and emission was collected through a 505-550 nm band pass filter. After concluding the experiments with Pal-car and Pal-CoA, pore-forming antibiotic alamethicin (10 μg/ml) was applied to induce maximal calcein release from the

mitochondrial matrix and the minimum calcein fluorescence after alamethicin is regarded as 0 % for the normalization of calcein fluorescence.

Measurement of ROS in skinned myocytes

For the measurement of ROS generation, permeabilized myocytes were loaded with a continuous perfusion of fluorescent indicator 2'7'-dichlorofluorescin diacetate (DCF: 10 μM). Cells were excited at 514 nm with an argon laser, and the emission signals were collected through a 530 nm long-pass filter. The fluorescent intensity at identical regions of interest (25 × 25 pixels) were monitored every 1 min to analyze changes in DCF signals.

Measurement of FAD oxidation

The mitochondrial redox state of single myocytes was assessed by measuring their FAD-linked protein fluorescence. Endogenous FAD auto-fluorescence was excited at 488 nm with an argon laser and fluorescence was collected through a 505 nm long-pass filter. Two-dimensional images were acquired at 1 min intervals. The FAD signal decreased to a minimum in the presence of cyanide (CN^-, 4 mM), an inhibitor of cytochrome oxidase, and increased upon exposure to the uncoupler of mitochondria, 2, 4-dinitrophenol (DNP, 100 μM). CN^- and DNP were expected to cause maximum reduction and oxidation (**9**), respectively. Each signal was calibrated as 0 % for

CN^--induced complete reduction and as 100 % for DNP. Fluorescence intensity was integrated over regions of interest (25 × 25 pixels) excluding the nuclei and the edge of the cell.

Chemicals and data analyses

All chemicals were obtained from Sigma (St Louis, MO, USA) and fluorescent dyes were purchased from Molecular Probes (Eugene, OR, USA). Data is presented as means ± SE, and the number of cells or experiments is shown as n. Statistical analyses were performed using two-way ANOVA of repeated measurements, followed by Bonferroni test. A level of $p<0.05$ was accepted as statistically significant.

Fatty acyl-carnitine and fatty acyl-CoA and inhibitors of CPT

Palmitoyl-L-carnitine (Pal-car) was dissolved in the internal solution and palmitoyl-CoA (Pal-CoA) was dissolved in ethanol. Ethanol was present in the perfused solution at a final concentration of 0.2 % and had no individual effect on TMRE, calcein, DCF or FAD intensity. In this study, we did not apply BSA to the solution, in order to avoid attenuating the activities of these fatty acyl intermediates in the solution (**13**). Perhexiline, a CPT-I and CPT-II inhibitor, and oxfenicine, a CPT-I inhibitor (**11**) were dissolved in the internal solution.

Results

Effects of Pal-car on $\Delta\psi_m$ and mPTP

We investigated the effects of Pal-car on $\Delta\psi_m$ and mPTP. Figure 1A demonstrates the time course of the changes in TMRE intensity, which represent the changes in mitochondrial $\Delta\psi_m$, during and after the application of Pal-car (1 to 10 μM) for 10 min. Pal-car (1 and 5 μM) slightly increased TMRE intensity (115.5 ± 5.4 % of the baseline, and 110.7±1.6 % of the baseline, respectively. $p<0.05$). However, higher concentration of Pal-car (10 μM) depolarized $\Delta\psi_m$ significantly (61.9 ± 12.2 % of the baseline, $p<0.01$). These results indicated that when appropriate concentrations of Pal-car were added in the internal solution and taken up by mitochondria, mitochondrial basal metabolism would be accelerated and $\Delta\psi_m$ was hyperpolarized slightly. On the other hand, the application of higher concentrations of Pal-car (and possibly higher concentrations of Pal-CoA inside the mitochondrial matrix and/or excessive Pal-car in the cytosol) results in $\Delta\psi_m$ depolarization. To differentiate this effect, the same experiments were conducted with perhexiline, a CPT-I and CPT-II inhibitor. When cells were pretreated with perhexiline (0.1 μM), subsequent application of Pal-car (1 μM in Figure 2A and 10 μM in Figure 2B) did not alter $\Delta\psi_m$, indicating that the observed

changes in $\Delta\psi_m$ were related to the uptake of Pal-car into the mitochondrial matrix and to its metabolism.

The opening of mPTP has been suggested to be a mechanism of FA-induced mitochondrial damage (**2**, **13**). We hypothesized that the opening of mPTP could be involved in Pal-car-induced $\Delta\psi_m$ depolarization. We have previously reported that the reduction of mitochondrial trapped calcein intensity indicates the opening of mPTP in permeabilized myocytes (**9**). Figure 1B demonstrates the changes in calcein intensity during and after 10 min perfusion of Pal-car. The pore-forming antibiotic alamethicin was applied after the perfusion of Pal-car to complete maximal release of calcein from the mitochondrial matrix, providing positive control. Application of 1 μM Pal-car did not cause any changes in calcein intensity (95.4 ± 2.9 % of the baseline) compared to the control. However, 10 μM Pal-car decreased calcein intensity significantly (70.7 ± 2.8 % of the baseline, $p<0.01$ vs. control). An mPTP inhibitor, cyclosporine A (CsA; 0.1 μM) attenuated Pal-car-induced reduction of calcein signal (84.5 ± 0.2 % of the baseline). From these results, it was shown that there were biphasic effects of Pal-car on $\Delta\psi_m$ and mPTP, that is, only higher concentrations of Pal-car depolarized $\Delta\psi_m$ and opened mPTP.

Effects of Pal-CoA on $\Delta\psi_m$ and mPTP

Under conditions of increased plasma free FA levels, the concentration of Pal-CoA in cytosolic space would also be increased (**30**). We next investigated the effects of Pal-CoA on $\Delta\psi_m$ and mPTP. In this series of experiments, cells were permeabilized and L-carnitine did not exist in the internal solution. Therefore, this suggested that Pal-CoA applied to the internal solution could not enter into the mitochondrial matrix since the conversion of Pal-CoA to Pal-car might not occur. Figure 3A shows the time course of the changes in TMRE intensity during 10 min perfusion of Pal-CoA (0.1 to 10 μM) and after the wash out. In contrast to Pal-car, Pal-CoA (0.1 to 5 μM) decreased TMRE signal at 10 min (90.8 ± 3.8 % with 0.1 μM, 84.7 ± 2.8 % with 0.5 μM, 65.8 ± 4.2 % with 1 μM, and 56.9 % ± 13.0 % with 5 μM, $p<0.05$ and $p<0.01$ vs. baseline) dose-dependently. However, when cells were exposed to a higher concentration of Pal-CoA (10 μM), $\Delta\psi_m$ dissipated rapidly and completely within a few minutes. These results suggest that the accumulation of Pal-CoA in the cytosolic space altered $\Delta\psi_m$, and the higher concentration of Pal-CoA might be harmful to the maintenance of mitochondrial function.

We next examined whether Pal-CoA could open mPTP by measuring the reduction of calcein intensity. The time course of the changes in calcein intensity in the

presence of Pal-CoA is shown in Figure 3B. In contrast to the effects of Pal-car on mPTP (Figure 1B), the reduction of calcein intensity by Pal-CoA (1 to 10 μM), which were the concentrations to depolarize $\Delta\psi_m$, was the same as that of the control perfusion. These results suggest that the depolarization or dissipation of $\Delta\psi_m$ by Pal-CoA is not related to the opening of mPTP.

Effects of Pal-car and Pal-CoA on the generation of ROS

It has been suggested that ROS generation is related to FA-induced mitochondrial damage and apoptosis (**29**) and that ROS was a potent inducer of mPTP opening (**7**). Figure 4 shows the time course of the changes in DCF intensity during and after the 10 min perfusion of Pal-car (1 and 10 μM) and Pal-CoA (10 μM). The data shows that 1 μM Pal-car promoted a gradual and modest increase (1.6 ± 0.2 fold of the baseline, $p<0.05$ vs. the baseline) in DCF fluorescence, and that the application of 10 μM Pal-car caused a rapid and larger increase (3.4 ± 0.3 fold of the baseline, $p<0.01$ vs. the baseline) in DCF intensity and DCF fluorescence decreased rapidly after the withdrawal of Pal-car. Since the decrease in DCF signal can not be due to the reduction of DCF by intracellular reductases and the efflux of oxidized DCF from mitochondria is dependent on ΔpH (membrane potential and proton gradient), a modest recovery of $\Delta\psi_m$ after Pal-car washout may have affected the efflux of this dye. In addition, a constant

perfusion of internal solution during protocols could wash out the leaked DCF immediately.

When cells were exposed to 10 μM Pal-car for 5 min, and then a ROS scavenger, N-acetylcysteine (NAC; 400 μM) (**21**), added to the internal solution in the continuous presence of 10 μM Pal-car, the increase in DCF intensity was completely eliminated, confirming that these changes in DCF fluorescence were attributed to the generation of ROS. In contrast to Pal-car, when cells were exposed to 10 μM Pal-CoA for 10 min, there was only a transient and slight increase in DCF signal (1.8 ± 0.2 fold of baseline, $p<0.05$ vs. the baseline) followed by the reduction of the signal. Thus, the mechanisms of ROS generation by Pal-car and Pal-CoA were shown to be different and that only the perfusion of Pal-car generated ROS significantly in the mitochondrial matrix.

MPTP inhibitor and ROS scavenger prevented Pal-car-induced $\Delta\psi_m$ depolarization

The changes in TMRE intensity with Pal-car (10 μM) in the presence of cyclosporine A (CsA), an mPTP inhibitor, are shown in Figure 5A. When cells were pretreated with CsA (0.1 μM), the reduction of TMRE intensity by Pal-car (10 μM) was notably inhibited (87.7 ± 6.2 % of baseline, $p<0.01$ vs. Pal-car alone). To further confirm that the mPTP-mediated depolarization of $\Delta\psi_m$ can be related to the generation of ROS, the effects of NAC on Pal-car-induced $\Delta\psi_m$ depolarization was investigated.

As shown in Figure 5B, pretreatment with NAC (400 μM) slightly increased (107 ± 3.0 % of baseline, $p<0.01$ vs. Pal-car alone) rather than decreased TMRE signals after the application of Pal-car (10 μM). These results indicate that both a CsA-sensitive opening of mPTP and ROS generation are related to the depolarization of $\Delta\psi_m$ induced by Pal-car under our experimental conditions.

Extra-mitochondrial Pal-CoA did not alter mitochondrial redox state

As shown in Figures 3A and 3B, Pal-CoA depolarized $\Delta\psi_m$ without opening mPTP. We then applied Pal-CoA and L-carnitine simultaneously to encourage the uptake of Pal-CoA into the mitochondrial matrix. When cells were pretreated with L-carnitine (2.5 mM) (**6**) and then exposed to 10 μM Pal-CoA simultaneously, the Pal-CoA-induced depolarization of $\Delta\psi_m$ was prevented significantly. In addition, this $\Delta\psi_m$ preventing effect of L-carnitine was inhibited by CPT-I inhibitor, oxfenicine (10 μM) (Figure 6A). These results indicated that the stimulation of mitochondrial Pal-CoA uptake with L-carnitine prevented the deleterious effects of extra-mitochondrial Pal-CoA.

Finally, we investigated how Pal-CoA depolarized $\Delta\psi_m$. Previous studies proposed several mechanisms for the depolarization of $\Delta\psi_m$ induced by Pal-CoA (**2**), such as the direct inhibition of the respiratory chain, the generation of ROS, and

increased proton leak. We have already shown that the application of Pal-CoA caused only a small and transient ROS generation (Figure 4). In this study, we assessed the activity of the respiratory chain by measuring FAD auto-fluorescence. Acceleration of the respiratory chain increases oxidation of FADH to FAD, resulting in the elevation of FAD auto-fluorescence. When myocytes were perfused with 10 μM Pal-CoA for 10 min, there were no changes in FAD auto-fluorescence (Figure 6B). These results suggest that, under our experimental conditions, the direct effect of Pal-CoA on the respiratory chain was unlikely.

Discussion

It is well established that an accumulation of excess FA in cardiac myocytes leads to cardiac lipotoxity, which is associated with the development of heart failure (**1, 38**). Since lipotoxity from the accumulation of long chain FA is specific for saturated FA (**15**), we investigated the effects of Pal-car and Pal-CoA, the intermediates of the most common saturated FA, on $\Delta\psi_m$, opening of mPTP, and the generation of ROS in saponin-treated permeabilized cardiac myocytes. In this study, we demonstrated that (1) lower concentrations of Pal-car caused a slight hyperpolarization of $\Delta\psi_m$, but did not open mPTP, (2) the higher concentration of Pal-car depolarized $\Delta\psi_m$ and opened mPTP, (3) Pal-CoA depolarized $\Delta\psi_m$ without opening mPTP, and (4) only the higher concentration of Pal-car increased ROS generation. These results indicate that there are different actions between Pal-car and Pal-CoA on mitochondrial function.

Previous studies examining the effects of long chain FA or their intermediates on mitochondrial function were conducted mainly using isolated mitochondria (**13**, **25**) or cultured cells (**32**, **37**). Compared to those experiments with isolated mitochondria, the use in this study of permeabilized myocytes provides an opportunity to examine mitochondrial function under more physiological circumstances (**14**), and allows the cytosolic concentration of Pal-car or Pal-CoA to be controlled without changing the

conditions of the extra-mitochondrial medium (i.e. cytosolic Ca^{2+}, ATP or other substrates) and intracellular architectures (**14, 27**). The concentrations of Pal-car (**18**, **20**) or Pal-CoA (**31**) used in this study were within the ranges reported in previous studies.

The effects of Pal-car on $\Delta\psi_m$ and mPTP

We demonstrated the biphasic effect of Pal-car on $\Delta\psi_m$, where only the higher concentration of Pal-car (10 μM) depolarized $\Delta\psi_m$, while lower concentrations of Pal-car (1 and 5 μM) hyperpolarized $\Delta\psi_m$ (Figure 1A). These effects of Pal-car were prevented with CPT inhibitor perhexiline (Figures 2A and 2B), which has been reported to inhibit both CPT-I and CPT-II (**11**). Since the inhibition of CPT-II blocked the conversion of Pal-car to Pal-CoA in the inner membrane, it is suggested that the observed changes in $\Delta\psi_m$ were indeed related to the uptake of Pal-car into the mitochondrial matrix and to its metabolism. It has been reported that, in the cytosolic space of rat ventricular myocytes, the concentration of Pal-car was 2-2.5 μM (**8**). After Pal-car enters the mitochondrial matrix and is re-converted to Pal-CoA, it can be oxidized and stimulates an electron transport. The hyperpolarization of $\Delta\psi_m$ could be due to the acceleration of the respiratory chain achieved from the optimal supply of Pal-CoA as an energy substrate (**17**). In the experiments on isolated mitochondria,

10 μM Pal-car has been used as the substrate for mitochondrial respiration. Differences in experimental conditions may explain these discrepancies.

We also demonstrated that 10 μM Pal-car decreased calcein intensity significantly, which was blocked by CsA (Figure 1B), suggesting that Pal-car (10 μM) opened mPTP. Since CsA also inhibited Pal-car-induced depolarization of $\Delta\psi_m$ (Figure 5A), the opening of mPTP could explain the depolarization of $\Delta\psi_m$ by a higher concentration of Pal-car. The direct action of Pal-car on mPTP has not been reported, although a previous study reported that much higher concentrations of Pal-car (at least 25 μM) was required to enhance its amphiphilic effect (**16**). However, when 10 μM Pal-car was introduced in the cytosolic space and the uptake of Pal-car into mitochondria matrix was inhibited by perhexiline, there were no changes in $\Delta\psi_m$ under our experimental conditions (Figure 2B). When a large amount of Pal-car enters the matrix, concentrated Pal-car itself could serve as an amphiphile to damage mitochondria. Since most Pal-car is converted rapidly to Pal-CoA, existing amounts of Pal-car are estimated to be less than 15 % of total carnitine in the mitochondrial matrix (**8**). It is, therefore, unlikely that excessive Pal-car, either inside or outside mitochondria, altered $\Delta\psi_m$ or opened mPTP directly.

The effects of Pal-CoA on $\Delta\psi_m$ and mPTP

Pal-CoA plus L-carnitine was applied to the internal solution in order to facilitate Pal-CoA transportation across the inner mitochondrial membrane, as cytosolic L-carnitine may not exist by itself after permeabilization of the plasma membrane. In this study, we showed that Pal-CoA depolarized $\Delta\psi_m$ (Figure 3A) and that the application of L-carnitine (**6**) with Pal-CoA inhibited the Pal-CoA-induced depolarization (Figure 6A), indicating that an excessive amount of extra mitochondrial Pal-CoA impairs mitochondrial function. These results are in good agreement with a previous study that demonstrated that L-carnitine has protective effects against mPTP and ischemia/reperfusion injury (**26**). It has been reported that when chronic substrate supply exceeds the capacity of oxidation or when the oxidation process is compromised, intracellular lipid metabolites accumulate, which leads to arrhythmia and contractile dysfunction (**22**, **23**).

Several mechanisms could be involved in the depolarization of $\Delta\psi_m$ induced by fatty acyl-CoA; (1) membrane peroxidation, (2) the direct inhibition of the respiratory chain, (3) opening mPTP, and (4) proton leaking effects (**2**). Fatty acyl-CoA inserts its hydrophobic moiety and binds to biological membranes because of its amphiphilic effect (**2**). Pal-CoA induces a peroxidation of the membrane at concentrations as low as

10 μM (**16**) and depolarizes $\Delta\psi_m$ due to amphiphilic properties outside mitochondria (**4**, **16**). Pal-CoA promotes mPTP opening by either (1) its interaction on adenine nucleotide translocase (ANT) increasing the probability of mPTP opening (direct effect) (**28**, **36**) or (2) its protonophoric effects depolarizes $\Delta\psi_m$ and it opens mPTP (indirect effect) (**2**, **13**).

In this study, Pal-CoA did not accelerate calcein leakage from mitochondria in spite of the complete dissipation of $\Delta\psi_m$ (Figures 3A and 3B). In addition, we did not observe any changes in FAD auto-fluorescence from Pal-CoA (Figure 6B), indicating that Pal-CoA did not alter the mitochondrial redox-state significantly, and that the inhibitory effect of Pal-CoA on the respiratory chain was not significant. Previous studies have reported on the protonophoric properties of long chain FA (**13**, **16**, **36**), and the strongest activity was found for C12-C16 saturated FA (**2**). However, fatty acyl-CoA does not exert protonophoric activity nor uncouple oxidative phosphorylation, because they are unable to cross the inner mitochondrial membrane and they do not flip-flop because of the large hydrophilic CoA head (**2**). Taken together, it is likely that Pal-CoA-induced depolarization or dissipation of $\Delta\psi_m$ could be due to the proton leaking effects of Pal-CoA acting from outside the mitochondria.

The effects of Pal-car and Pal-CoA on ROS generation

In this study, we demonstrate that Pal-car increased ROS generation (Figure 4) and that NAC prevented the depolarization of $\Delta\psi_m$ (Figure 5B), suggesting the contribution of Pal-car-induced ROS generation to the opening of mPTP. On the other hand, Pal-CoA caused ROS generation only for a short period and total amounts of ROS were significantly smaller compared with those of Pal-car. The distinct responses of ROS generation caused by FA intermediates has not previously been reported and this is the first study to demonstrate that there are significant differences between Pal-car and Pal-CoA induced ROS generation in skinned myocytes.

The mechanism of mitochondrial ROS generation induced by FA remains to be clarified. Several studies reported that direct inhibition of the respiratory chain was attributed to ROS generation by FA (**13**, **32**). Schönfeld and Wojtczak (**29**) reported that FA abolishes ROS generation in rat heart mitochondria when electron transport was reversed. As Pal-car supplies electrons and stimulates (rather than inhibits) the mitochondrial respiratory chain (**29**), it is postulated that the acceleration of electron transport might contribute, at least in part, to Pal-car-induced ROS generation under our experimental conditions. It has been reported that a transient increase in ROS triggers a burst generation of ROS in neighboring mitochondria (ROS-induced ROS-release;

RIRR) (**39**). This RIRR may explain the rapid and larger increase in DCF fluorescence caused by Pal-car observed in this study. Pal-CoA may alter the mitochondrial membrane structure by its amphiphilic properties (**3**) and generated ROS may cause peroxidation of the mitochondrial membrane (**16**). These structural and functional changes could be responsible for the observed Pal-CoA-induced ROS generation. It has also been reported that Pal-CoA could stimulate ROS generation by inhibiting ANT (**13**). Further studies are required to identify the distinct mechanism of mitochondrial ROS generation between Pal-car and Pal-CoA.

Clinical implication

In patients with metabolic disorders, such as metabolic syndrome, obesity, and diabetes mellitus (**19**), cardiac lipotoxity has been implicated in the pathogenesis of clinical heart failure as a result of enhanced FA metabolism secondary to elevated serum FA (**15**). Recent clinical studies using positron emitted tomography (PET) techniques have provided evidence of higher myocardial FA uptake ratios in patients with heart failure (**34**) and an increased FA utilization and accumulation of FA that could lead to myocardial dysfunction (**1**, **2**). Our results suggest that the excessive exogenous intermediates of long chain saturated FA may disturb mitochondrial function in different ways between Pal-car and Pal-CoA. These findings may be useful to

establish strategies for the treatment of heart failure caused by the impairment of FA metabolism.

Conclusion

This study demonstrates that excessive amounts of Pal-car, which could result in an inappropriate increase of Pal-CoA in the mitochondrial matrix, are harmful to mitochondrial function by accelerating ROS production and by increasing the probability of opening mPTP. On the other hand, an excessive cytosolic Pal-CoA itself may affect mitochondrial function by causing a loss of $\Delta\psi_m$ from outside the mitochondria. These distinct mechanisms of the deteriorating effects of long chain FAs on mitochondrial function are important for our understanding of the development of cardiac diseases in systemic metabolic disorders.

Acknowledgements

This work was supported by Japan Grant in Aid 13670703 (to H.K) and 50135258 (to H.H), and by Grant Aid for the Center of Excellence (COE) from the Ministry of Education, Culture, Sports, Science, and Technology (Japan).

References

1. **Ashrafian H, Frenneaux MP, Opie LH.** Metabolic mechanisms in heart failure. *Circulation* 116: 434-448, 2007.

2. **Bernardi P, Penzo D, Wojtczak L.** Mitochondrial energy dissipation by fatty acids. Mechanisms and implications for cell death. *Vitam Horm* 65: 97-126, 2002.

3. **Boylan JG, Hamilton JA.** Interactions of acyl-coenzyme A with phosphatidylcholine bilayers and serum albumin. *Biochemistry* 31: 557-567, 1992.

4. **Brecher P.** The interaction of long-chain acyl CoA with membranes. *Mol Cell Biochem* 57: 3-15, 1983.

5. **Chiu HC, Kovacs A, Blanton RM, Han X, Courtois M, Weinheimer CJ, Yamada KA, Brunet S, Xu H, Nerbonne JM, Welch MJ, Fettig NM, Sharp TL, Sambandam N, Olson KM, Ory DS, Schaffer JE.** Transgenic expression of fatty acid transport protein 1 in the heart causes lipotoxic cardiomyopathy. *Circ Res* 96: 225-233, 2005.

6. **Faergeman NJ, Knudsen J.** Role of long-chain fatty acyl-CoA esters in the regulation of metabolism and in cell signalling. *Biochem J* 323: 1-12, 1997.

7. **Halestrap AP, McStay GP, Clarke SJ.** The permeability transition pore complex: another view. *Biochimie* 84: 153-166, 2002.

8. **Idell-Wenger JA, Grotyohann LW, Neely JR.** Coenzyme A and carnitine distribution in normal and ischemic hearts. *J Biol Chem* 253: 4310-4318, 1978.

9. **Katoh H, Nishigaki N, Hayashi H.** Diazoxide opens the mitochondrial permeability transition pore and alters Ca^{2+} transients in rat ventricular myocytes. *Circulation* 105: 2666-2671, 2002.

10. **Kenchaiah S, Evans JC, Levy D, Wilson PW, Benjamin EJ, Larson MG, Kannel WB, Vasan RS.** Obesity and the risk of heart failure. *N Engl J Med* 347: 305-313, 2002.

11. **Kennedy JA, Kiosoglous AJ, Murphy GA, Pelle MA, Horowitz JD.** Effect of perhexiline and oxfenicine on myocardial function and metabolism during low-flow ischemia/reperfusion in the isolated rat heart. *J. Cardiovasc. Pharmacol* 36: 794-801, 2000.

12. **Kerner J, Hoppel C.** Fatty acid import into mitochondria. *Biochim Biophys Acta* 1486: 1-17, 2000.

13. **Korge P, Honda HM, Weiss JN.** Effects of fatty acids in isolated mitochondria: implications for ischemic injury and cardioprotection. *Am J Physiol Heart Circ Physiol* 285: H259-269, 2003.

14. **Lesnefsky EJ, Moghaddas S, Tandler B, Kerner J, Hoppel CL.** Mitochondrial dysfunction in cardiac disease: ischemia/reperfusion, aging, and heart failure. *J Mol Cell Cardiol* 33: 1065-1089, 2001.

15. **Listenberger LL, Han X, Lewis SE, Cases S, Farese RV, Jr., Ory DS, Schaffer JE.** Triglyceride accumulation protects against fatty acid-induced lipotoxicity. *Proc Natl Acad Sci USA* 100: 3077-3082, 2003.

16. **Mak IT, Kramer JH, Weglicki WB.** Potentiation of free radical-induced lipid peroxidative injury to sarcolemmal membranes by lipid amphiphiles. *J Biol Chem* 261: 1153-1157, 1986.

17. **Marin-Garcia J, Goldenthal MJ.** Fatty acid metabolism in cardiac failure: biochemical, genetic and cellular analysis. *Cardiovasc Res* 54: 516-527, 2002.

18. **Maruyama K, Hara A, Hashizume H, Ushikubi F, Abiko Y.** Ranolazine attenuates palmitoyl-L-carnitine-induced mechanical and metabolic derangement in the isolated, perfused rat heart. *J Pharm Pharmacol* 52: 709-715, 2000.

19. **Masoudi FA, Inzucchi SE.** Diabetes mellitus and heart failure: epidemiology, mechanisms, and pharmacotherapy. *Am J Cardiol* 99: 113B-132B, 2007.

20. **Mutomba MC, Yuan H, Konyavko M, Adachi S, Yokoyama CB, Esser V, McGarry JD, Babior BM, Gottlieb RA.** Regulation of the activity of caspases by L-carnitine and palmitoylcarnitine. *FEBS Lett* 478: 19-25, 2000.

21. **Nagasaka S, Katoh H, Niu CF, Matsui S, Urushida T, Satoh H, Watanabe Y, Hayashi H.** Protein kinase A catalytic subunit alters cardiac mitochondrial redox state and membrane potential via the formation of reactive oxygen species. *Circ J* 71: 429-436, 2007.

22. **Oliver MF, Kurien VA, Greenwood TW.** Relation between serum-free-fatty acids and arrhythmias and death after acute myocardial infarction. *Lancet* 1: 710-714, 1968.

23. **Oliver MF, Opie LH**. Effects of glucose and fatty acids on myocardial ischaemia and arrhythmias. *Lancet* 343: 155-158, 1994.

24. **Opie LH.** The metabolic vicious cycle in heart failure. *Lancet* 364: 1733-1734, 2004.

25. **Penzo D, Tagliapietra C, Colonna R, Petronilli V, Bernardi P**. Effects of fatty acids on mitochondria: implications for cell death. *Biochim Biophys Acta* 1555: 160-165, 2002.

26. **Reznick AZ**, **Kagan VE**, **Ramsey R**, **Tsuchiya M**, **Khwaja S**, **Serbinova EA**, **Packer L**. Antiradical effects in L-propionyl carnitine protection of the heart against ischemia-reperfusion injury: the possible role of iron chelation. *Arch Biochem Biophys.* 296: 394-401, 1992.

27. **Saotome M, Katoh H, Satoh H, Nagasaka S, Yoshihara S, Terada H, Hayashi H.** Mitochondrial membrane potential modulates regulation of mitochondrial Ca^{2+} in rat ventricular myocytes. *Am J Physiol Heart Circ Physiol* 288: H1820-1828, 2005.

28. **Schönfeld P, Bohnensack R.** Fatty acid-promoted mitochondrial permeability transition by membrane depolarization and binding to the ADP/ATP carrier. *FEBS Lett* 420: 167-170, 1997.

29. **Schönfeld P, Wojtczak L.** Fatty acids decrease mitochondrial generation of reactive oxygen species at the reverse electron transport but increase it at the forward transport. *Biochim Biophys Acta* 1767: 1032-1040, 2007.

30. **Sharma S, Adrogue JV, Golfman L, Uray I, Lemm J, Youker K, Noon GP, Frazier OH, Taegtmeyer H.** Intramyocardial lipid accumulation in the failing human heart resembles the lipotoxic rat heart. *FASEB J* 18: 1692-1700, 2004.

31. **Siliprandi D, Biban C, Testa S, Toninello A, Siliprandi N.** Effects of palmitoyl CoA and palmitoyl carnitine on the membrane potential and Mg^{2+} content of rat heart mitochondria. *Mol Cell Biochem* 116: 117-123, 1992.

32. **Sparagna GC, Hickson-Bick DL, Buja LM, McMillin JB.** A metabolic role for mitochondria in palmitate-induced cardiac myocyte apoptosis. *Am J Physiol Heart Circ Physiol* 279: H2124-2132, 2000.

33. **Stanley WC, Recchia FA, Lopaschuk GD.** Myocardial substrate metabolism in the normal and failing heart. *Physiol Rev* 85: 1093-1129, 2005.

34. **Taylor M, Wallhaus TR, Degrado TR, Russell DC, Stanko P, Nickles RJ, Stone CK.** An evaluation of myocardial fatty acid and glucose uptake using PET with [^{18}F] fluoro-6-thia-heptadecanoic acid and [^{18}F] FDG in Patients with Congestive Heart Failure. *J Nucl Med* 42: 55-62, 2001.

35. **Varela-Roman A, Grigorian Shamagian L, Barge Caballero E, Mazon Ramos P, Rigueiro Veloso P, Gonzalez-Juanatey JR.** Influence of diabetes on the survival of patients hospitalized with heart failure: a 12-year study. *Eur J Heart Fail* 7: 859-864, 2005.

36. **Weiss JN, Korge P, Honda HM, Ping P.** Role of the mitochondrial permeability transition in myocardial disease. *Circ Res* 93: 292-301, 2003.

37. **Xiao YF, Kang JX, Morgan JP, Leaf A.** Blocking effects of polyunsaturated fatty acids on Na^+ channels of neonatal rat ventricular myocytes. *Proc Natl Acad Sci USA* 92: 11000-11004, 1995.

38. **Zhou YT, Grayburn P, Karim A, Shimabukuro M, Higa M, Baetens D, Orci L, Unger RH.** Lipotoxic heart disease in obese rats: implications for human obesity. *Proc Natl Acad Sci USA* 97: 1784-1789, 2000.

39. **Zorov DB, Juhaszova M, Sollott SJ.** Mitochondrial ROS-induced ROS release: an update and review. *Biochim Biophys Acta* 1757: 509-517, 2006.

Figure legends

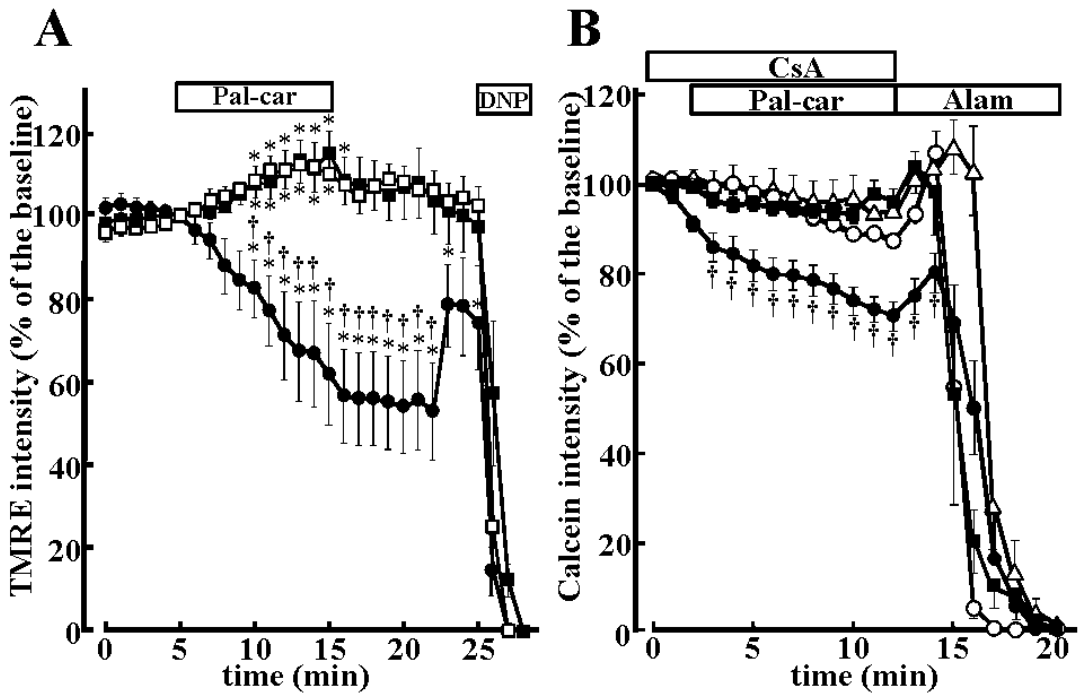

Figure 1

Palmitoyl-L-carnitine (Pal-car) depolarized $\Delta\psi_m$ and opened mPTP

(A) Effects of Pal-car on $\Delta\psi_m$: The time course of the changes in TMRE intensity during and after 10 min perfusion of Pal-car. Sarcolemmal membrane of rat cardiac myocytes was permeabilized by 0.05 mg/ml of saponin, and then, as indicated by the bars at the top, permeabilized myocytes were exposed to 1-10 μM of Pal-car (1 μM; ■, n=8, 5 μM; □, n=5, 10 μM; ●, n=9) for 10 min in a Ca^{2+}-free internal solution. Pal-car was removed by the continuous perfusion of a Ca^{2+}-free internal solution. As a reference, an uncoupler DNP (100 μM) was applied at the end of the experiments. Data is presented as the % of TMRE intensity before Pal-car application (* $p<0.05$ vs. the baseline, † $p<0.01$ vs. 1 or 5 μM Pal-car, by two-way ANOVA and Bonferroni test).

(B) Effects of Pal-car on calcein intensity: The time course of the changes in calcein signals during and after 10 min perfusion of Pal-car. As indicated by the bars at the top, saponin-permeabilized myocytes were exposed to 1-10 μM of Pal-car (control; △, n=15, 1 μM; ■, n=7, 10 μM; ●, n=7) for 10 min in a Ca^{2+}-free internal solution. In CsA treated cells, CsA (0.1 μM) was pretreated for 2 min to inhibit the mPTP opening, and then 10 μM Pal-car was perfused in the presence of CsA (○; n=7). After 10 min perfusion of Pal-car or Pal-car plus CsA, the pore-forming antibiotic alamethicin was applied for the complete reduction of calcein intensity, providing a positive control of maximal calcein release from the mitochondrial matrix. Data is normalized with the baseline (100 %) and alamethicin-induced minimum calcein intensity (0 %). († $p<0.01$ vs. control, by two-way ANOVA and Bonferroni test).

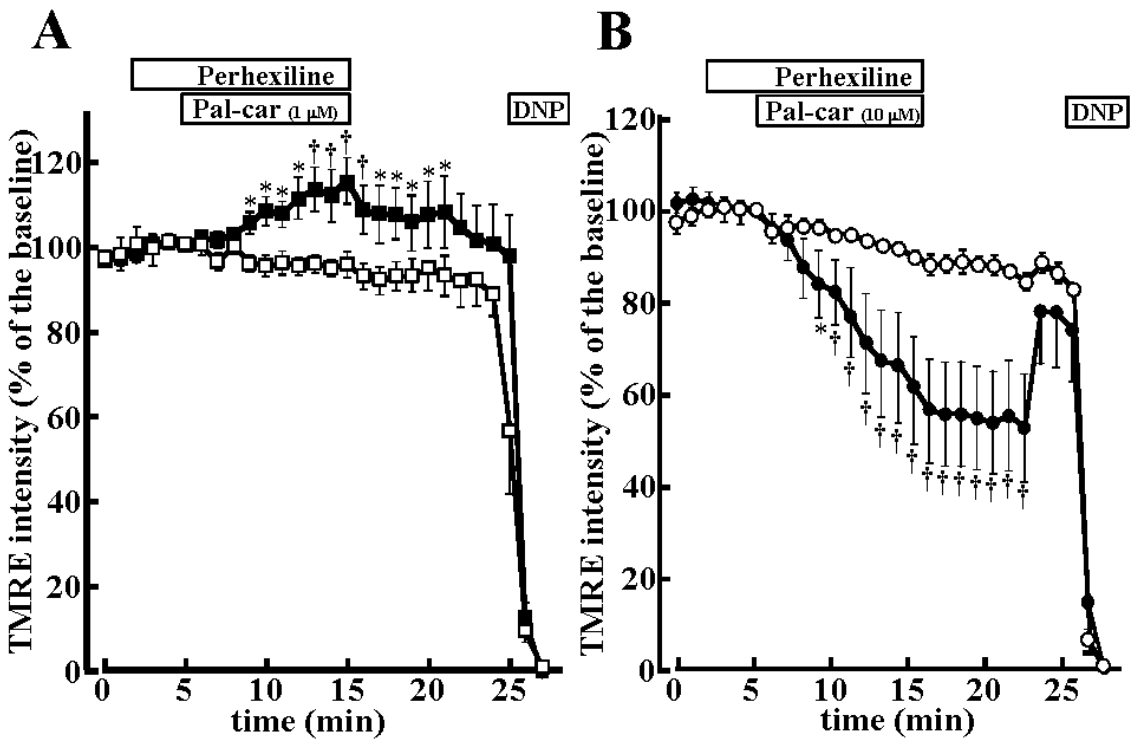

Figure 2

Perhexiline inhibited Pal-car-induced changes in $\Delta\psi_m$

(A) The time course of the changes in TMRE signals during and after 10 min perfusion of Pal-car (1 μM): Permeabilized myocytes were exposed to Pal-car (1 μM, ■, n=8) for 10 min in a Ca^{2+}-free internal solution. In a perhexiline (PHX) treated group, after 3 min pretreatment of perhexiline (0.1 μM), cells were exposed to Pal-car (1 μM) in the presence of perhexiline (□, n=6) for 10 min. Then, Pal-car and PHX were removed by a continuous perfusion of a Ca^{2+}-free internal solution. As a reference, DNP (100 μM) was applied at the end of experiments. Data is presented as % the of the baseline TMRE intensity. Values are means ± SE. († $p < 0.01$, Pal-car vs. Pal-car + PHX, * $p < 0.05$, Pal-car vs. Pal-car + PHX, by two-way ANOVA and Bonferroni test)

(B) The same protocol was conducted with 10 μM Pal-car: '■' represents Pal-car (n=8) and '○' represents Pal-car + PHX (n=6). Values are means ± SE. († $p < 0.01$, Pal-car vs. Pal-car + PHX, * $p < 0.05$, Pal-car vs. Pal-car + PHX, by two-way ANOVA and Bonferroni test)

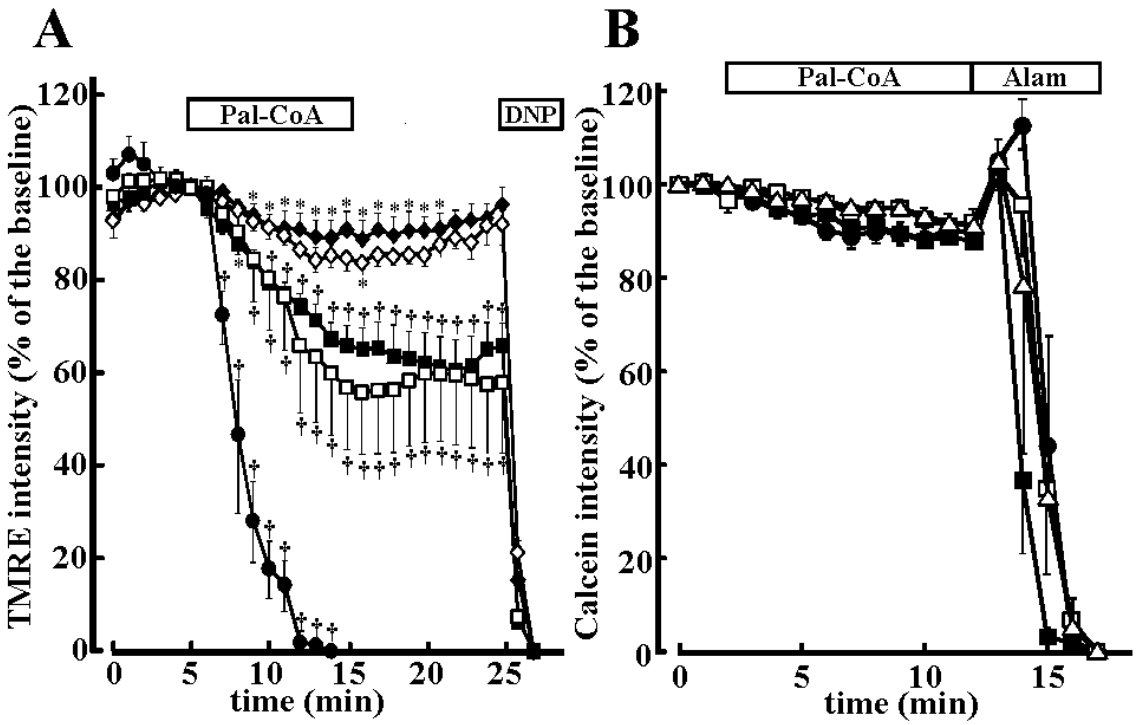

Figure 3

Palmitoyl-CoA (Pal-CoA) depolarized $\Delta\psi_m$ but did not open mPTP

(A) Effects of Pal-CoA on $\Delta\psi_m$: The time course of the changes in TMRE intensity during and after 10 min perfusion of Pal-CoA. The permeabilized cells were exposed to 0.1-10 μM of Pal-CoA (0.1 μM; ◆, n=8, 0.5 μM; ◇, n=13, 1 μM; ■, n=11, 5 μM; □, n=8, 10 μM; ●, n=4) for 10 min in a Ca^{2+}-free internal solution as indicated by the bars at the top. Pal-CoA was removed by the perfusion of a Ca^{2+}-free internal solution. As a reference, an uncoupler DNP (100 μM) was applied at the end of the experiments. Data is presented as the % of TMRE intensity before Pal-CoA application (* $p<0.05$ vs. the baseline, † $p< 0.01$ vs. the baseline by two-way ANOVA and Bonferroni test).

(B) Effects of Pal-CoA on calcein intensity: The time courses of the changes in calcein signals during and after 10 min perfusion of Pal-CoA. (△; control; n=15). Cells were perfused with 1 μM (■; n=4), 5 μM (□; n=12) and 10 μM (●; n=10) Pal-CoA. After 10 min perfusion of Pal-CoA, alamethicin was applied for a positive control of maximal calcein release from the mitochondrial matrix. Data is normalized with baseline (100 %) and alamethicin-induced minimum calcein intensity (0 %).

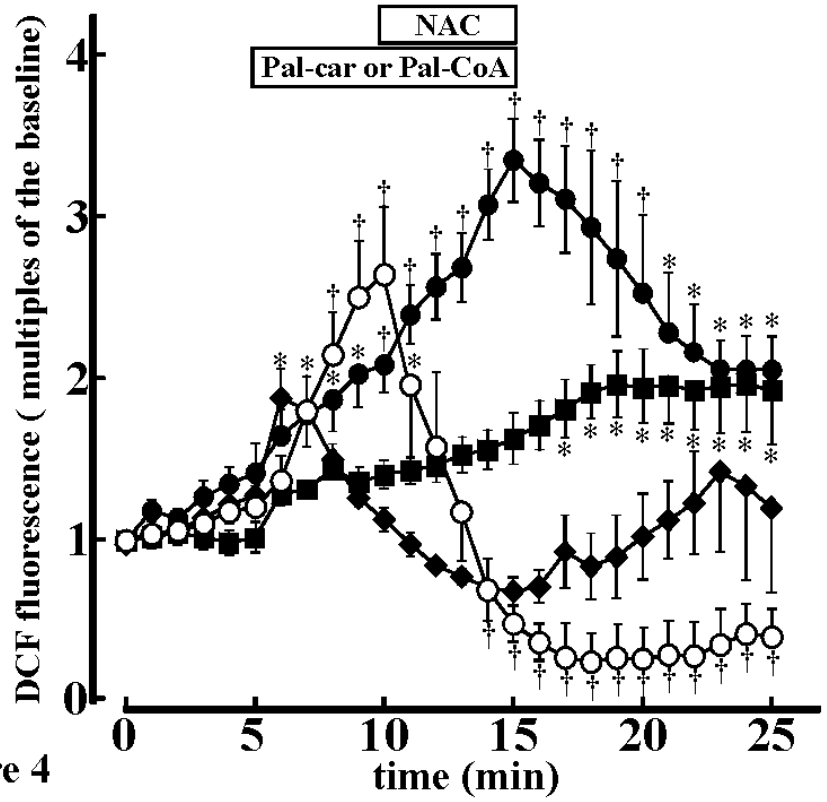

Figure 4

Pal-car accelerated ROS generation, but Pal-CoA did not

The time course of the changes in DCF fluorescence during and after the application Pal-car (1 μM; ■, n=8, 10 μM; ●, n=11) or Pal-CoA (10 μM; ◆, n=4) for 10 min as indicated in the bar. Pal-car or Pal-CoA was removed by a continuous perfusion of a Ca^{2+}-free internal solution. In N-acetylcysteine (NAC)-treated cells, NAC (400 μM) was added to the solution 5 min after the perfusion of Pal-car (10 μM) (Pal-car + NAC; ○, n=5) in order to scavenge ROS. Data is presented as multiples of the baseline before Pal-car or Pal-CoA application (* $p<0.05$ vs. the baseline, † $p<0.01$ vs. the baseline, by two-way ANOVA and Bonferroni test).

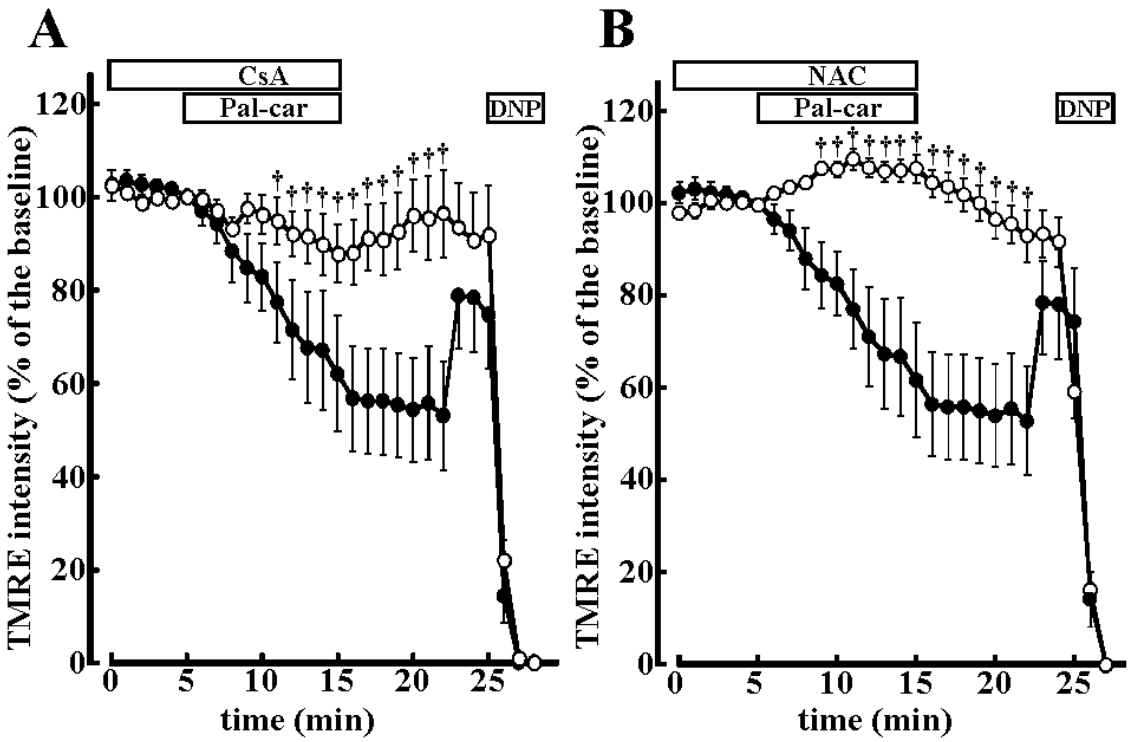

Figure 5

CsA and NAC inhibited Pal-car-induced $\Delta\psi_m$ depolarization

(A) Effects of CsA on Pal-car-induced $\Delta\psi_m$ depolarization: The time course of the changes in TMRE intensity by Pal-car (10 μM) in the absence (●; n=9) and presence of CsA (○, n=7). Cells were pretreated with CsA (0.1 μM) for 5 min, and then Pal-car was applied in the presence of CsA as indicated by the bars at the top. Pal-car or CsA were removed by the perfusion of a Ca^{2+}-free internal solution. As a reference, DNP (100 μM) was applied at the end of the experiments. Data is presented as the % of TMRE intensity before Pal-car application († $p< 0.01$, by two-way ANOVA and Bonferroni test).

(B) Effects of NAC on Pal-car-induced $\Delta\psi_m$ depolarization: The time course of the changes in TMRE intensity by Pal-car (10 μM) in the absence (●; n=9) and presence of NAC (○; n=12). Cells were pretreated with NAC (400 μM) for 5 min, and then Pal-car was added to the solution in the continuous presence of NAC for 10 min as indicated by the bars at the top. As a reference, DNP (100 μM) was applied at the end of the experiments. Data is presented as the % of TMRE intensity before Pal-car application († $p<0.01$, by two-way ANOVA and Bonferroni test).

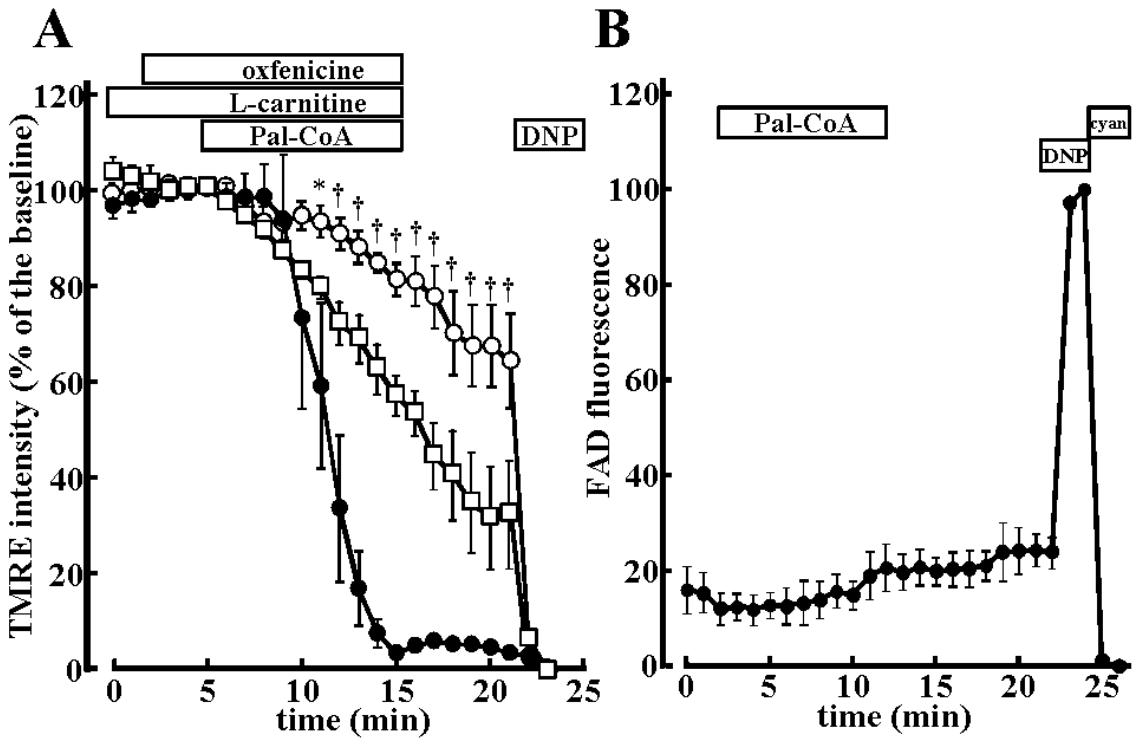

Figure 6

(A) ***L-carnitine prevented Pal-CoA-induced $\Delta\psi_m$ depolarization***

The time course of changes in TMRE intensity by Pal-CoA in the absence (●; n=5) and presence of L-carnitine (○; n=6). Cells were pretreated with L-carnitine (2.5 mM) for 5 min, and then Pal-CoA (10 μM) was applied for 10 min in the continuous presence of L-carnitine as indicated by the bars at the top. Pal-CoA and L-carnitine were removed by the perfusion of a Ca^{2+}-free internal solution. In the oxfenicine (OXF) treated group, cells were perfused with OFX (10 μM) 3 min before the application of Pal-CoA (□; n=7). As a reference, DNP (100 μM) was applied at the end of the experiments. Data is presented as the % of TMRE intensity before Pal-CoA application († $p<0.01$ vs. Pal-CoA alone by ANOVA and Bonferroni test).

(B) ***Pal-CoA did not alter FAD auto-fluorescence***

The time course of the changes in FAD signal during and after 10 min application of Pal-CoA (10 μM) in permeabilized myocytes (●; n=5). As indicated in the bar, at the end of the experiments, DNP (100 μM) and sodium cyanide (cyan: 4 mM) were applied as the references. Data are presented as the % of normalized FAD signal; i.e. referred to as 100 % for DNP -induced maximum oxidation and as 0 % for cyanide-induced reduction.